AJNR

MR and CT of Occult Vascular Malformations of the Brain

Paul F. J. New, Robert G. Ojemann, Kenneth R. Davis, Bruce R. Rosen, Roberto Heros, Raymond N. Kjellberg, Raymond D. Adams and E. P. Richardson

AJNR Am J Neuroradiol 1986, 7 (5) 771-779
http://www.ajnr.org/content/7/5/771

MR and CT of Occult Vascular Malformations of the Brain

Paul F. J. New[1]
Robert G. Ojemann[1]
Kenneth R. Davis[1]
Bruce R. Rosen[1]
Roberto Heros[1]
Raymond N. Kjellberg[1]
Raymond D. Adams[2]
E. P. Richardson[3]

The need for improved specificity in the diagnosis of "occult" vascular malformations led to the use of MR in suspected cases in order to determine MR's potential for improved diagnostic accuracy. Six patients with six lesions histologically diagnosed as vascular malformation after partial (1) or complete (5) microsurgical excision were studied by CT, MR, and selective magnification subtraction angiography. In all cases, the cerebral lesions were apparently solitary and were visible as focal lesions on both CT and MR. Since angiography failed to reveal the pathologic blood vessels of the lesions, and no arteriovenous shunting was evident, these lesions were termed vascular malformations occult to angiography (VMOTA). Angiography revealed a mass effect in only two cases. MR did not reveal additional vascular malformations missed by CT. In each case, MR, which was performed in an attempt to support the diagnosis suggested by CT, did in fact do so by revealing signal abnormalities indicative of nonacute hemorrhage within the lesion on T1- and T2-weighted pulse sequences. Although, as on CT, MR features of these lesions were found to be nonspecific, the MR criteria reinforced the probable diagnosis of VMOTA in an additional 30 cases that had shown similar nonspecific CT features. In this second group, excluded from this study, in which histologic verification was not obtained because of perceived hazards of surgery, the increased assurance regarding the diagnosis led to proton-beam therapy without histologic verification in 18 cases. It is concluded that MR can provide significant improvement in the accuracy of diagnosing VMOTA beyond that obtainable just by plain and contrast-enhanced CT.

Extensive experience with CT has led to the recognition of criteria for the diagnosis of vascular malformations occult to angiography (VMOTA) [1–8]. All varieties of vascular malformation have been identified in this group; arteriovenous malformations, cavernous malformations, venous malformations, and telangiectases [5, 8]. On plain CT, these lesions tend to present as hyperdense, or occasionally isodense, relatively small mass lesions, generally no more than 3 cm in diameter [8–11], often containing recognizable punctate or small dense foci indicative of areas of calcification. After intravenous contrast enhancement, relatively mild or moderate rather than marked enhancement is commonly seen. Occasionally, small regions of intense enhancement suggest the presence of contrast medium in small blood vessels. Although the CT features may be highly suggestive of the diagnosis, there is as a rule uncertainty in the differential diagnosis of these lesions from neoplasms, particularly low-grade astrocytomas and oligodendrogliomas. Granulomatous lesions may also show similar CT appearances and, rarely, avascular meningiomas may mimic VMOTAs. Because of the problems of accurate diagnosis, MR has been used at this center for approximately 2 years when this diagnosis has been suspected. This report documents our findings in six cases with surgical and histologic verification.

Subjects and Methods

Six patients for whom the diagnosis of a VMOTA was a major consideration were studied

This article appears in the September/October 1986 issue of *AJNR* and the November 1986 issue of *AJR*.

Received December 16, 1985; accepted after revision March 19, 1986.

Presented in part at the annual meeting of the American Society of Neuroradiology, San Diego, January 1986.

[1] Department of Radiology, Massachusetts General Hospital and Harvard Medical School, Boston, MA 02114. Address reprint requests to P. F. J. New, Dept. of Radiology, Section of Neuroradiology, Massachusetts General Hospital, Boston, MA 02114.

[2] Service of Neurology, Massachusetts General Hospital and Harvard Medical School, Boston, MA 02114.

[3] Department of Pathology (Charles S. Kubik Laboratory for Neuropathology), Massachusetts General Hospital and Harvard Medical School, Boston, MA 02114.

***AJNR* 7:771–779, September/October 1986**
0195–6108/86/0705–0771

TABLE 1: **Clinical, Surgical, and Histologic Features**

Case	Gender Age (yrs)	Site	Clinical	Surgery	Gross Appearance	Histology
1	M 26	L posterior temporal	3 mo. episodic headache, nausea and vomiting, difficulty reading	Excision	Encapsulated mass Old clot Gliosis	Vascular malformation
2	M 41	L pontocerebellar	1½ mo. episodic instability, dizziness, nausea, visual blurring	Excision	Tangle of vessels Gliosis, hematoma Cavity Thrombosed arteriovenous malformation	Arteriovenous malformation
3	M 27	Posterior pontomesencephalic	36 mo. episodic blurred vision, diplopia, headache, speech difficulty	Limited excision ventricular shunt	Encapsulated mass within old hemorrhage Thrombosed vascular malformation	Consistent with vascular malformation
4	M 40	L para-fourth ventricular	12 mo. episodic vertigo, nausea and vomiting, headache, diplopia, subarachnoid hemorrhage	Excision	Small mass Old hemorrhage Thrombosed arteriovenous malformation	Arteriovenous malformation
5	F 31	L frontal	8 mo. episodic minor seizures, recent generalized seizure	Excision	Encapsulated mass containing old hemorrhage Gliosis Vascular malformation	Arteriovenous malformation
6	F 40	L frontal	Many years of L frontal headache. 16 mo. earlier acute headache, nausea and vomiting, then obtundation, grand mal seizure	Excision	Localized mass Recent and old hemorrhage Gliosis Vascular malformation	Arteriovenous malformation

Note.—L = left.

by MR. CT was the initial imaging study in all cases and was performed using a variety of third- and fourth-configuration scanners, before and after intravenous contrast injection in all cases. Serial film selective catheter angiography, with magnification and subtraction, which in all cases failed to reveal either intrinsic abnormal vessels or vascular shunting, was performed either before or after MR. MR was performed using a superconductive whole-body system (Teslacon, Technicare Corp., Solon, OH) operating at 0.6 T (25.4 MHz). T1- and T2-weighted spin-echo (SE) pulse sequences and inversion recovery (IR) with spin-echo sequences were used. All patients had IR sequences with repetition times (TR) of 1500 or 1650 msec, inversion time (TI) of 400 or 450 msec, and echo time (TE) of 32 msec. Four acquisitions were averaged, except in one case, in which only a single acquisition was obtained. It is our usual practice to image the brain using the more T1-weighted IR sequence in preference to a short TR and TE SE sequence. One patient also had a less T1-weighted sequence, with TR 500 msec and TE 30 msec. One patient had in addition a mixed T1- T2-weighted SE sequence, TR 1500, TE 30. T2-weighted sequences were dual-echo SE 2000/60 and /120 msec, TR/TE, with four acquisitions, except for one patient who was examined with separate SE 1500/30 and 1500/60 sequences instead. The latter patient was examined with a single-section technique and 8-mm thick sections. The other patients all had multisection contiguous 7.5-mm slice technique. All patients were studied with axial sections. One patient had an additional IR sequence in the sagittal plane.

Data were acquired with 128-line resolution in the phase-encoded (Y) axis, interpolated to 256, and 256 lines in the frequency-encoded (X) axis, for a display matrix of 256 mm^2, giving pixel resolution of 2.0×1.0 mm.

Clinical Features

There were four men and two women, ranging in age from 26 to 41 years (mean, 34.1 years). In general, the predominant symptoms were similar to those described in earlier reports [3, 8]. Symptoms were typically episodic, over weeks, months, or years, and most frequently consisted of headache, with or without nausea and vomiting, seizures of various types, and focal neurologic deficits appropriate to the region involved (Table 1).

CT and MR

In each case, the pre- and postcontrast attenuation characteristics revealed by CT, and the signal intensities and their patterns on T1- and T2-weighted images, were analyzed and compared with those of normal anatomic structures shown in the same CT section and in the same MR image. T1 and T2 relaxation values were assessed qualitatively and were not measured or calculated.

Angiography

All angiograms were performed by selective catheterization, with magnification and subtraction. The examinations were all restudied retrospectively.

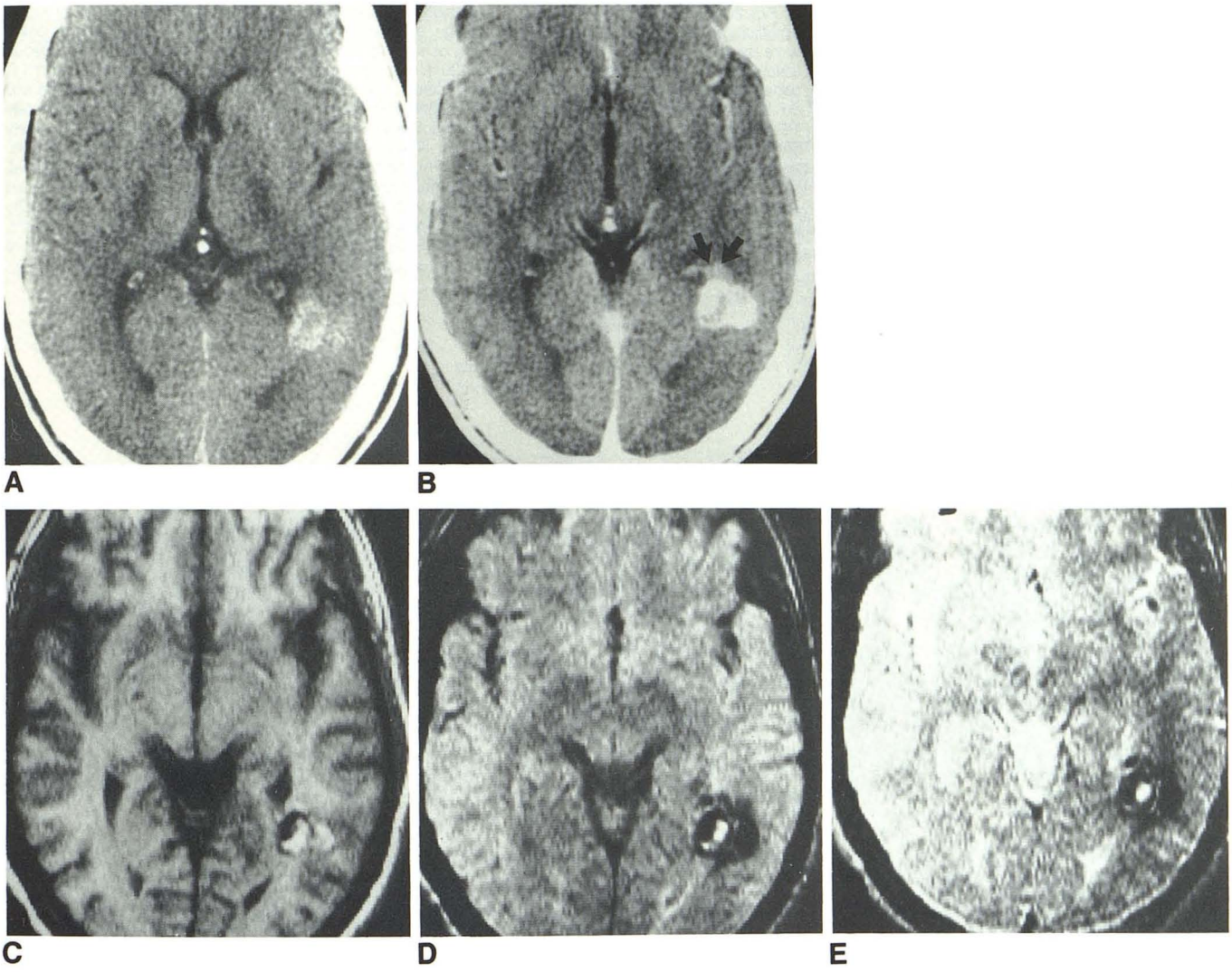

Fig. 1.—Case 1. **A**, Plain CT shows heterogeneous hyperdense lesion adjacent to trigone and occipital horn, probably but not definitely including punctate calcifications. **B**, After contrast, there is moderate heterogeneous enhancement of lesion, with appearance of small vessels anteriorly (*arrows*). Small vessels were apparent in lateral portion of lesion at time of acute hemorrhage 2½ months earlier (not shown). **C**, MR, 4 days later. IR 1650/450/32/4. Bright islands indicating short T1 are partly surrounded by areas of absent or near-absent signal. **D**, SE 2000/60/2 moderately T2-weighted sequence shows smaller bright islands of prolonged T2 within more extensive region of absent signal. **E**, Same sequence, but with TE 120. The bright foci are smaller than in **D**, but there is little change in appearance of surrounding area of signal void.

Results

Angiography

Each case satisfied the strict criteria for VMOTA in that no pathologic vessels or arteriovenous shunting were identified on careful retrospective study of the angiograms. There was no evidence of mass effect in four cases, and mass effect was identified in two cases.

CT

The lesions in all patients were 3 cm or less in diameter. All showed somewhat heterogeneous hyperdensity relative to brain on plain CT. In only two cases (cases 3 and 6) was definite granular calcification identified. In the lesions of three other cases (cases 1, 2, and 4), the heterogeneous hyperdensity raised suspicion of punctate calcifications, nonacute hemorrhage, dense soft tissues, or a combination of these. Case 5 had an isodense appearance, without mass effect on initial plain CT. Four months later, CT showed an irregular, thick ring with the density of relatively recent hemorrhage, and a lower mixed density centrally. The pattern suggested hemorrhage in a neoplasm, rather than a vascular malformation. In case 1, plain CT originally revealed a focal acute hemorrhage in the left temporal lobe, and intravenous contrast enhancement produced a slight increase in density at the periphery of the hematoma. Focal areas of this enhancement were consistent with small associated blood vessels. Two and a half months later, plain CT revealed a heterogeneous hyperdense lesion at the same site, and moderate, slightly heterogeneous enhancement occurred. There was again indication of small abnormal blood vessels in the region. In all

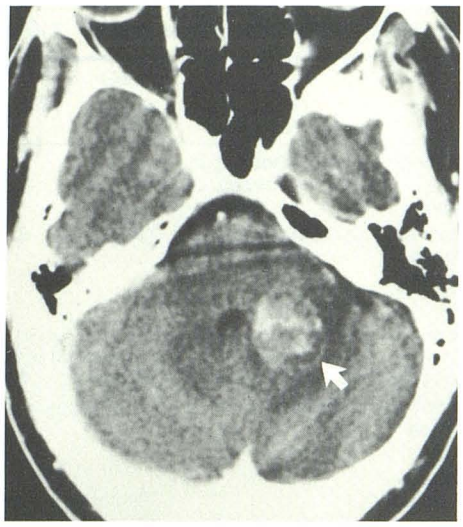

A

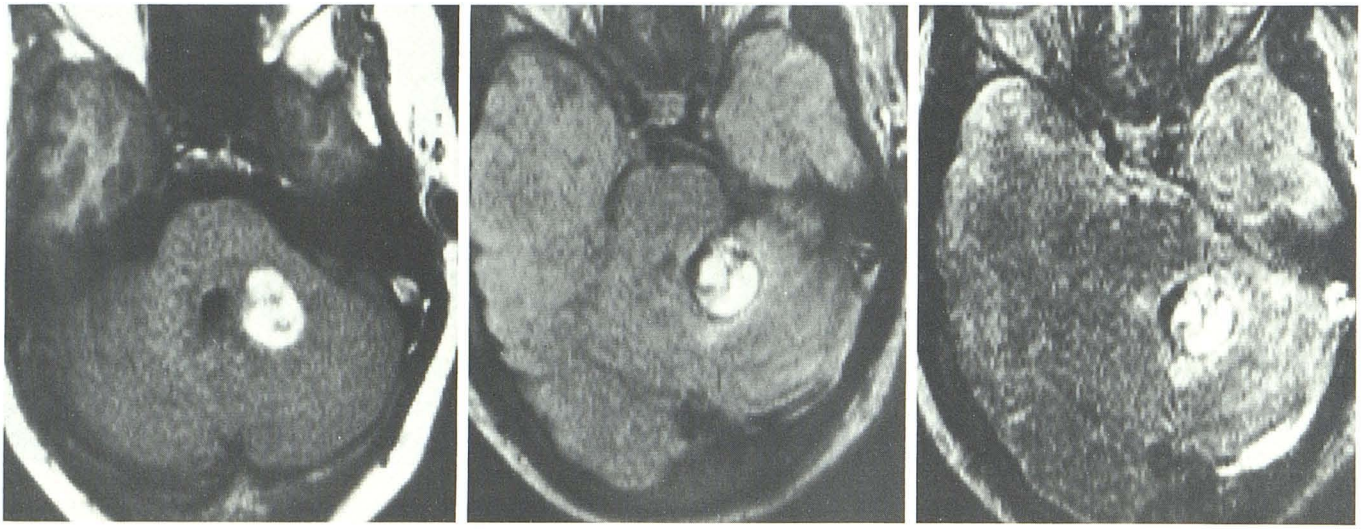

B C D

Fig. 2.—Case 2. **A**, Contrast CT shows moderate irregular enhancement of lesion, centered in left brachium pontis. In this and an adjacent section, enhancement of small vessels in and adjacent to lesion were seen (e.g., *arrow*). Noncontrast scan (not shown) revealed a heterogeneous, largely hyperdense lesion. **B**, MR, 2 days after CT, IR 1650/450/20/4, reveals largely homogeneous bright signal of short T1, consistent with nonacute hemorrhage. Areas of lesser signal centrally are consistent with hemorrhage and do not correspond to areas of enhancement suggestive of vessels on CT. **C**, SE 2000/60/4 moderately T2-weighted sequence 7.5 mm higher than section **B** shows large bright islands of increased T2, largely bounded by zone of absent signal and irregular areas of absent or reduced signal between the islands. With same SE sequence as at level in **B** (not shown), there was a narrow, almost completely circumferential, zone of absent signal around high signal. Posteriorly and laterally, a less intense signal around the lesion is indicative of edema. **D**, The same sequence, but with TE 120, more markedly T2-weighted. High-intensity islands and peripheral absent signal are much the same in distribution as in **C.** Perifocal edema is evident. Note that low signal regions between bright islands do not show appreciable increase in intensity (lack of second echo enhancement) and therefore are not suggestive of slowly flowing blood within vessels.

lesions, enhancement was mild or moderate in degree and heterogeneous in pattern. However, small rounded or arcuate foci of marked enhancement appeared in three cases (cases 1, 2, and 4), indicating the presence of small abnormal blood vessels (Figs. 1, 2, and 4; Table 2).

In summary, the findings on CT fitted well with the variety of appearances previously reported in VMOTA [1–8]. After angiography, VMOTA was the suspected diagnosis in all but cases 5 and 6, in which a hemorrhagic neoplasm (case 5) and a partially calcified glioma (case 6) were strongly suspected.

MR

Of the six cases, T1- weighted images revealed one or more foci of short T1, appearing as one or more bright "islands" in four cases (Figs. 1 and 2). Cases 4 and 6 showed only low signal (Figs. 3 and 4). In addition, areas of very low or absent signal on T1-weighted images were present peripherally and/or centrally in four cases and questionable in a fifth.

On T2-weighted images, one or more foci on long T2, appearing as one or more bright "islands," were seen in five cases. This was accompanied by very low or absent T2 signal (very short T2) in five cases, was arranged peripherally in four cases, and peripherally plus centrally in one case ("dark lakes"). In the remaining case (case 6), the entire area showed low to absent T2 signal (Fig. 4, Table 2).

Surgery

The lesion was excised partially in case 3 and completely in the remaining five cases, using microsurgical techniques. The gross appearance of the lesion at surgery was described as thrombosed arteriovenous malformation in cases 2 and 4 and as "vascular malformation" in the remaining cases.

All lesions appeared well encapsulated and showed gross evidence of old hemorrhage in cases 1–5 and of old and recent hemorrhage in case 6. Hemosiderin deposition was specifically commented upon in cases 5 and 6.

TABLE 2: **CT and MR Findings, and Time Intervals**

Case	CT		Interval to MR	MR			Interval to Surgery
	Plain	Enhanced		T1 Weighted	T2 Weighted	More T2 Weighted	
1	Acute hemorrhage 2½ mo. earlier; now hyperdense	Small vessels; moderate CE + small vessels	4 days	Confluent bright foci; adjacent signal void	Smaller bright islands within larger signal void	Same except smaller bright islands	4 weeks
2	Hyperdense	Mild to moderate CE + small vessels	2 days	Bright island; less intense area within	Bright islands; peripheral signal void	Same	2 days
3	Hyperdense; granular calcifications	Mild to moderate CE	21 weeks + multiple over 4½ yrs. postop. (unchanged)	Confluent bright islands, most within low or absent signal	Similar confluent bright islands; more obvious peripheral and central signal void	Similar	243 weeks after limited excision
4	Hyperdense, with some hypodensity	Mild CE + small vessels	9 days	Small focus of low signal (< gray matter)	Island of isointense signal within signal void	Lesion obscured by noise	3 days
5	Isodense 4 mo. earlier; now recent hemorrhage, peripheral denser than central	Moderate CE adjacent to recent hemorrhage	Same day	Large bright island; small central low signal focus	Bright island; narrow peripheral interrupted void	Not done	2 days
6	Hyperdense; granular calcifications	Mild CE	11 weeks	Low signal (< gray matter) only	Low signal and void	Larger signal void	5 weeks

Note.—CE = contrast enhancement.

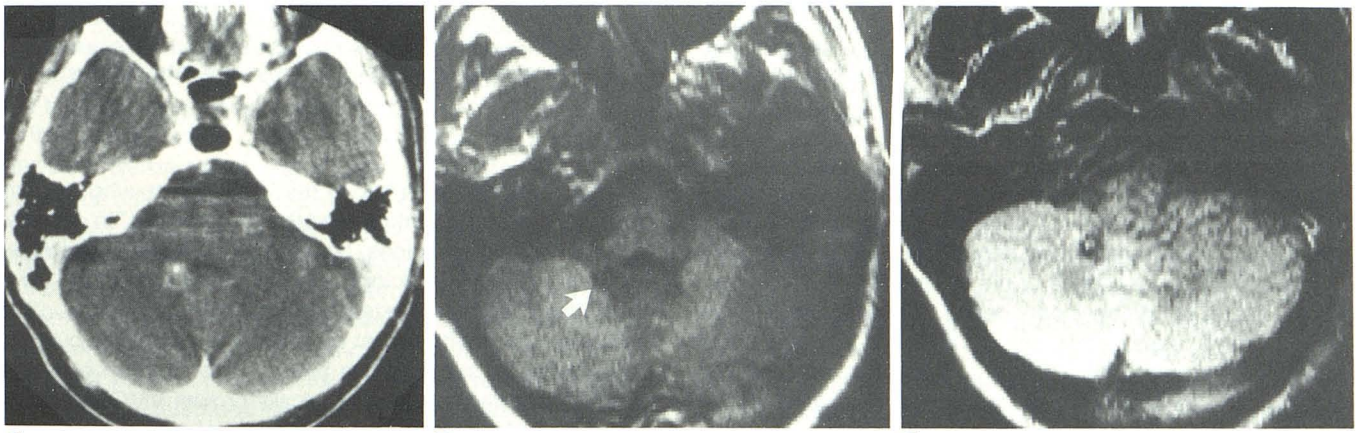

Fig. 3.—Case 4. **A**, Contrast-enhanced scan showing mild enhancement of this small, hyperdense lesion. One area of high density and a posterior arc of slightly increased density both suggest opacification of small blood vessels. Plain CT (not shown) showed mixed hyper- and hypodensity without definite calcification. The mass encroaches slightly upon the fourth ventricle. **B**, MR, 8 months later. IR 1500/450/4 T1-weighted section slightly below the level in **A**. There is small region of prolonged T1, similar to the T1 of gray matter, projecting into inferior portion of right cerebellar corpus medullaris from inferior vermis (*arrow*). No focus of short T1 is visible, presumably because hemorrhage was now many months old. **C**, SE 2000/60/2 moderately T2-weighted sequence at same level as **B.** A small area of approximately isointense signal is surrounded by zone of absent or near-absent signal. On same sequence with TE 120, no definite abnormality could be detected in this region, apparently because of the much higher noise level. (Note similarity to Fig. 5.)

Histology

Surgically excised material from each lesion was carefully reviewed. Because of the fragmentary character of the small tissue samples available, it was difficult to categorize with complete assurance the precise type of vascular malformation present in each case, although when viewed in light of the appearance at surgery, there was no doubt that these all represented vascular malformations. In various combinations, the following histologic features were observed: abnormally

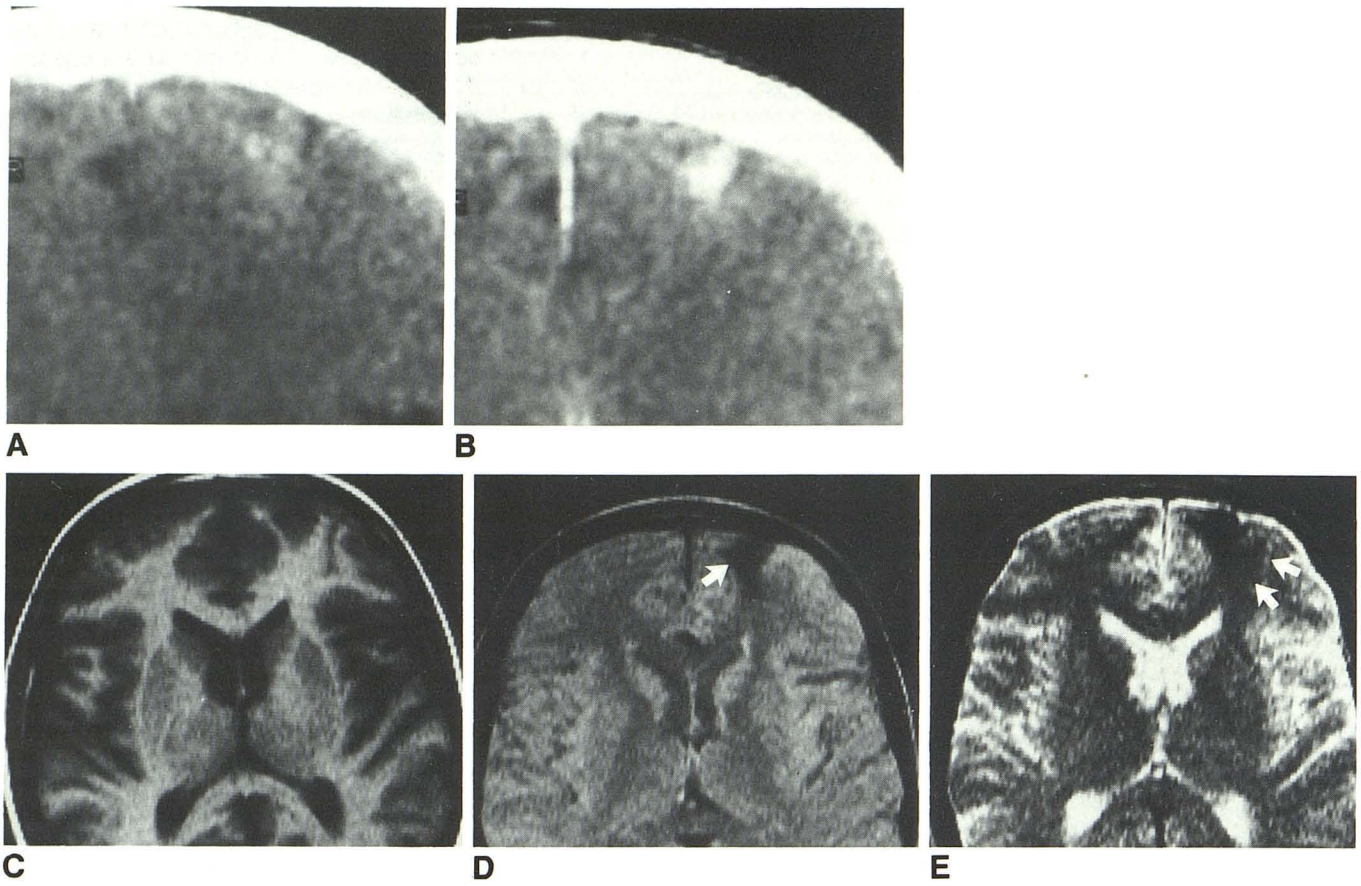

Fig. 4.—Case 6. **A**, Plain CT shows small hyperdense region in anterior left frontal lobe region, involving the cortex. Small granular calcifications are apparent. **B**, After intravenous contrast, area shows mild contrast enhancement surrounding calcifications. MR was performed 3 months after CT. **C**, IR 1500/450/4 sequence. A region of low signal, indicating T1 somewhat longer than gray matter, is shown extending from cortex into subcortical white matter. No mass effect is evident. **D**, SE 2000/60/2. The region of lesion (*arrow*) shows slightly heterogeneous pattern of absent to near-absent signal, indicating shortened T2, which is now confirmed by absent signal shown in **E** (*arrows*), obtained with a more strongly T2-weighted sequence, 2000/120/2. The lesion was excised 5 weeks later, when a little recent hemorrhage was identified in addition to much old clot and hemosiderin. It is probable that further hemorrhage occurred after MR.

formed blood vessels, many thrombosed or fibrosed; hyalinization of the walls of abnormal vessels; dystrophic calcifications; gliosis and hemosiderin deposition, frequently in high concentration; and evidence of old or recent and old hemorrhage (Table 1). Hemosiderin deposition was identified in tissue from all cases except case 1. Although the lesion was completely excised, only tiny fragments were available for microscopy. The final histologic diagnosis was arteriovenous malformation in one case, consistent with arteriovenous malformation in four cases, and vascular malformation of indeterminant type in one case (Table 1).

Discussion

Small vascular malformations became widely recognized after the report of Margolis et al. in 1951 [9], in which they called attention to small vascular malformations found on autopsy of six patients. Four of these were associated with fatal hemorrhage. Crawford and Russell [10] found that small vascular malformations were responsible for 20 of 461 cases of intracerebral hemorrhage. No abnormal vasculature was seen on angiography in two of the four patients who had this study. These authors introduced the term "cryptic" to describe these small malformations, because of their latent character both clinically and pathologically. Since that time, there have been many reports of arteriovenous malformations or other vascular malformations that were angiographically occult and responsible for spontaneous hemorrhage. Hashim et al. [8] recently reported three histologically proven VMOTAs. They were able to find only 47 reported cases of such histologically proven arteriovenous malformations not associated with clinically recognizable intracranial hemorrhage. The majority of these cases presented with seizures of various types and some with headaches. The lesions were generally detected by CT. Other vascular malformations with similar presentations have also been reported and include cavernous angiomas and venous angiomas [4, 5]. From previous reports, it is evident that VMOTAs are generally small, less than 2–3 cm in maximum size [8–11]. The true incidence is unknown, but their ratio to the classical malformations was 48:5, as detected in 48 autopsied cases by McCormick and Nofzinger [11]. They are usually said to give rise to signs and symptoms

when they hemorrhage, and hemorrhage may be massive. These lesions may present with neurologic symptoms without clinical evidence of intracranial hemorrhage. This was the case in each of our six cases, although the CT obtained at the time of a clinical exacerbation provided clear evidence of recent hemorrhage in two cases (cases 1 and 5). In the other four cases, CT did not reveal evidence of recent hemorrhage, owing either to failure to obtain CT at the appropriate time or to the presence of only a small seepage of recent hemorrhage, indistinguishable from the background hyperdensity of the VMOTA.

MR is steadily gaining acceptance as an important addition to the array of imaging techniques available for the investigation of neurologic disease, and it has been proposed as the diagnostic imaging method of choice for many forms of intracranial disease [12–15]. The capacity of MR to depict normal and abnormal vascular structures with high image contrast, without the need for intravascular contrast agents, has been demonstrated for normal vessels and a variety of vascular lesions [16–19]. A small number of cases has been reported in which intracranial vascular malformations have been identified by MR [20, 21]. A recent report of the comparative evaluation of CT and MR in 24 patients with 29 cerebral vascular malformations included 15 vascular malformations (in 11 patients) in which angiography revealed no pathologic circulation (VMOTAs) [20]. Histologic confirmation of the diagnosis was available in five of the 11 patients with VMOTAs. Ten of the 15 lesions could be seen equally well on CT and MR, three were more conspicuous on MR, and two were more conspicuous on CT. In the other six cases, the lesions were not safely accessible to biopsy or excision. Inherent hyperdensity was present on CT in 11 of the 15 lesions, and nonspecific enhancement, usually minimal, occurred in 13 lesions. Thirteen of 15 lesions were detected with MR, and the two that were missed were shown on CT only by virtue of fine punctate calcifications. Those that were shown by MR revealed relative signal void in three, hemorrhage in 12, and peripheral edema in seven. Evidence of slow flow (even-echo rephasing) could not be seen in any lesion. The regions of signal void were punctate or globular in all cases and were attributed to calcification rather than to high flow in vessels. However, the one illustrated case (Fig. 4) revealed a signal void much larger than the focus of calcification shown on CT and there were no corresponding opacified vessels. We suggest that the illustrated signal void in that case, and in our cases, is therefore most consistent with the selective effect of paramagnetic "clumps" (in this case hemosiderin deposits in macrophages) on spin-echo signal intensity. This manifests as a selective decrease in the apparent T2 of the region imaged, with lesser T1 effect. This phenomenon differs from that of the more commonly discussed interaction of uniformly distributed paramagnetic ions in solution (dipolar coupling), which affects T1 more strongly.

The effect we observe relates to the induction of local variations in the induced magnetic field (bulk susceptibility) by paramagnetic hemosiderin of the tissue under study. Paramagnetic materials, in addition to coupling directly to protons to increase relaxation rates, also have substantial fields induced when placed in a large external field; that is, they have large magnetic susceptibilities. This is due to the unpaired electron spins of the paramagnetic material, and the fields induced are much larger than those within normal, diamagnetic tissues. Clumps of paramagnetic substances, such as hemosiderin, would thus serve locally to distort the magnetic field "seen" by surrounding water protons. When water molecules diffuse through variations in magnetic field, their protons pick up phase changes that are not corrected for by the application of 180° refocusing pulses, since the field seen by a given proton is not constant with time. This results in a decrease in spin-echo signal intensity and would be observed as a decrease in the measured T2. This effect does not influence longitudinal relaxation, and hence a selective decrease in observed T2 is expected. This is in fact what was observed. The TE of 32 msec in the IR imaging introduces a T2 component, which can account for the absent signal regions on the T1-weighted images. Experience indicates that there is usually insufficient dense calcification in these lesions to produce sufficiently marked decrease in mobile proton density to explain signal void regions.

Kucharczyk et al. [20] conclude that at present CT detects VMOTAs more sensitively when faint calcification is the major evidence of their presence and MR is more accurate in evaluating associated hemorrhages, particularly when these have lost density with time or when they are located in the posterior fossa. Our experience conforms with these conclusions.

Lee et al. [21] included five cases of VMOTA, all in the posterior fossa. Two were verified by surgery. Hyperintense signal consistent with hemorrhage was shown on T1- and T2-weighted images in four cases. Multiple areas of decreased signal were shown within the hematomas in all these cases, and a curvilinear decreased signal was shown around the hematomas in three cases. In an additional case, a similar low signal was shown by the same pulsing techniques in a lesion having no evidence of hematoma. CT demonstrated increased attenuation in all five cases, with values consistent with calcification in only one case. They illustrate three cases of brainstem VMOTAs that have peripheral (three cases) and peripheral and central (two cases) very low signal intensity. This does not appear compatible with the presence of vascular signal voids, because the appearance and size of the signal-void regions do not correspond to the small size of vessels and the slow flow present in VMOTAs. In only one case was CT also illustrated, and this showed areas of calcific density that did not correspond to peripheral signal void on MR.

Studies in the first report cited above [20] were obtained at 0.35 T; those in the second report [21], at 0.5 T. The possibility of paramagnetic effects producing the low signal-to-signal void components of these lesions are not mentioned by either group. It has been stated that paramagnetic proton preferential T2 relaxation effects increase as the square of the magnetic field [22], and that certain paramagnetic effects are not likely to be shown by MR at lower field strengths (circa and below 0.5 T). It is possible that preferential T2 relaxation was not observed as regularly or prominently in

A B C

Fig. 5.—Multiple metastases of malignant melanoma, in which CT some time earlier had indicated neoplasm with probable hemorrhagic components. One of the multiple similar-appearing lesions in cerebellum and brainstem is illustrated here on paramedian sagittal sections. **A**, SE 500/30/4, mildly T1-weighted image, showing a low to absent signal in medial portion of cerebellar hemisphere. **B**, SE 2000/60/4, moderately T2-weighted sequence. There is a region of absent signal surrounding a small island that is isointense with cerebellar gray matter. **C**, SE 2000/120/4, strongly T2-weighted sequence, showing a small, intense focus of prolonged T2 within a region of low to absent signal. Note similarity to lesion shown in Figure 3.

the series reported by Kucharczyk et al. [20] or Lee et al. [21] for them to consider that this phenomenon was a plausible explanation for the low to absent signal regions associated with VMOTAs, rather than calcifications or vessels with high flow rates. Hemosiderin is a physiologically available paramagnetic relaxant, with a locally heterogeneous field varying slowly or not at all, and capable of producing locally heterogeneous magnetic susceptibility and local field gradients under the influence of a strongly applied magnetic field.

It is therefore our hypothesis that the regions of very low to absent signal described and illustrated in the above two reports [20, 21] and in our cases are due in fact to paramagnetic effects or magnetic susceptibility and not to vascular flow or to calcification. In our cases, the morphology of both the small vessels seen and the calcification, identified with certainty in only two cases, could not explain the patterns of signal void on MR.

Our results confirm the inability of CT to identify older parenchymal hemorrhages and add to a growing recognition that MR can reveal relatively characteristic and specific signal alterations (short T1, long T2) in nonacute hematomas [12, 22–27]. The short T1, believed to be due to the paramagnetic effect of methemoglobin, appearing after the first few days following hemorrhage and lasting for several months [28], represents an important advance over CT in imaging lesions consisting of or containing subacute and/or chronic hemorrhage. A feature corroborating hemorrhage, the appearance of absent or near-absent signal, presumed to be due to the magnetic susceptibility effect of hemosiderin, appears to be characteristic of lesions in which there has been considerable previous hemorrhage on one or more occasions. The presence of this signal pattern further helps characterize a hemorrhagic lesion in the type of case in which there is no clinical episode to suggest the occurrence of hemorrhage, such as in the present series of VMOTAs. This is presumably due to relatively slow seepage of small amounts of blood from relatively small vessels carrying slow flow under low pressure.

Although CT cannot always differentiate clusters of tiny calcifications from relatively dense soft tissues, slowly flowing blood, or blood clot, it can often distinguish small punctate or aggregated calcifications. Such small calcifications can generally not be identified by MR [29, 30]. With CT, the appearance of slight to moderate enhancement of these lesions is helpful in differential diagnosis, since low-grade gliomas, the principal differential consideration, generally do not show this type of enhancement. Nevertheless, since old hemorrhage cannot be identifed on CT, when angiography fails to reveal a pathologic circulation, it has been necessary in the past to undertake surgical confirmation by open operation or stereotactic biopsy, or to elect to perform serial CT scans over a protracted period.

Stereotactic biopsy is hazardous, since these occult lesions are prone to hemorrhage after this procedure with potentially fatal results [31]. Some deeply situated VMOTAs present at a ventricular surface (as in cases 2 and 4) and may be excisable by careful microsurgery [32], with low morbidity. However, many of these deep-seated lesions are not amenable to safe, open surgical exploration. Therefore, the unequivocal demonstration of significant previous hemorrhage or hemorrhages in these lesions by MR may provide greater assurance regarding the correct diagnosis, offering the opportunity of improved, particularly safer, patient management. In deeply seated lesions, not surgically accessible without undue hazard, the combination of typical findings on MR as well as by CT, may offer a better rationale for proton-beam therapy [33], without histologic confirmation. This approach was used in 18 of the initial 30 patients with clinical, CT, and MR features of VMOTA, in whom surgery of any type was judged to be unduly hazardous. Most of the lesions so treated involved the brainstem.

CT remains a necessary part of the evaluation of VMOTAs for the following reasons: follow-up CT a short time after an acute parenchymal hemorrhage will generally provide evidence that there is an underlying lesion (residual heterogeneous hyperdensity, with or without small calcifications, the opacification of very small intrinsic vascular channels in a

VMOTA, or evidence of an underlying neoplasm, particularly metastatic malignant melanoma or necrosing glioblastoma). These contributions to differential diagnosis are exemplified by our case 1 and by a case of hemorrhage into metastatic cerebellar melanoma (Fig. 5). In the latter case, the MR abnormalities of the individual lesions in themselves might not have provided the correct diagnosis. Low-grade gliomas may show small calcifications, but are unlikely to hemorrhage. Such a glioma may dedifferentiate, undergo necrosis, and thus become liable to hemorrhage. After hemorrhage, MR alone might not allow distinction from VMOTA, whereas CT can generally provide indication of underlying neoplasm by revealing a neoplastic pattern of contrast enhancement as the density of hemorrhage decreases. However, in case 5, both CT and MR suggested a hemorrhagic neoplasm.

We conclude from this study that CT and MR have complementary positions in the evaluation of suspected VMOTA.

Addendum

Since this report was completed, two further operated cases and one autopsied case (death from massive pontine hemorrhage from the VMOTA) showed CT and MR features similar to the six cases reported herein.

ACKNOWLEDGMENTS

We thank Paul Beaulieu, Bradley Field, and Maryann Kotowski for technological assistance, and Edith Bell for manuscript preparation.

REFERENCES

1. Kramer RA, Wing SD. Computed tomography of angiographically occult cerebral vascular malformations. *Radiology* **1977**;123:649–652
2. Bell BA, Kendall BE, Symon L. Angiographically occult arteriovenous malformations of the brain. *J Neurol Neurosurg Psychiatry* **1978**;41:1057–1064
3. Shuey HM Jr., Day AL, Quisling RG, Sypert GW. Angiographically cryptic cerebrovascular malformations. *Neurosurg* **1979**;5(4):476–479
4. Becker DH, Townsend JJ, Kramer RA, Newton TH. Occult cerebrovascular malformations. A series of 18 histologically verified cases with negative angiography. *Brain* **1979**;102:249–287
5. Cohen HCM, Tucker WS, Humphreys RP, Perrin RJ. Angiographically cryptic histologically verified cerebrovascular malformations. *Neurosurg* **1982**;10(6):704–714
6. Yeates A, Enzmann D. Cryptic vascular malformations involving the brainstem. *Radiology* **1983**;146:71–75
7. Mitnick JS, Pinto RS, Lin JP, Rose H, Lieberman A. CT of thrombosed arteriovenous malformations in children. *Radiology* **1984**;150:385–389
8. Hashim ASM, Asakura T, Koichi U, et al. Angiographically occult arteriovenous malformations. *Surg Neurol* **1985**;23:431–439
9. Margolis G, Odom GL, Woodhall B, et al. The role of small angiomatous malformations in the production of intracerebral hematomas. *J Neurosurg* **1951**;8:564–575
10. Crawford JV, Russell DS. Cryptic arteriovenous and venous hamartomas of the brain. *J Neurol Neurosurg Psychiatry* **1956**;19:1–11
11. McCormick WF, Nofzinger JD. "Cryptic" vascular malformations of the central nervous system. *J Neurosurg* **1966**;24:865–875
12. Bydder GM, Steiner RE, Young IR, et al. Clinical NMR imaging of the brain: 140 cases. *AJNR* **1982**;3:459–480, *AJR* **1982**;139:215–236
13. Brant-Zawadzki M, Davis PL, Crooks LE, et al. NMR demonstration of cerebral abnormalities: comparison with CT. *AJNR* **1983**;4:117–124, *AJR* **1983**;140:847–854
14. Bradley WG, Waluch V, Yadley RA, Wycoff RR. Comparison of CT and NMR in 400 patients with suspected disease of the brain and cervical spinal cord. *Radiology* **1984**;152:695–702
15. Lee BCP, Kneeland JB, Cahill PT, Deck MDF. MR recognition of supratentorial tumors. *AJNR* **1985**;6:871–878
16. Crooks LE, Mills CM, Davis PL, et al. Visualization of cerebral and vascular abnormalities by NMR imaging: the effects of imaging parameters on contrast. *Radiology* **1982**;144:843–852
17. Kaufman L, Crooks LE, Sheldon PE, et al. Evaluation of NMR imaging for detection and quantification of obstructions in vessels. *Invest Radiol* **1982**;17:554–560
18. Herfkens RJ, Higgins CB, Hricak H, et al. Nuclear magnetic resonance imaging of the cardiovascular system: normal and pathologic findings. *Radiology* **1983**;147:749–759
19. Bradley WG, Waluch V, Lai K, et al. The appearance of rapidly flowing blood on magnetic resonance images. *AJR* **1984**;143:1167–1174
20. Kucharczyk W, Lemme-Pleghos L, Uske A, Brant-Zawadzki M, Dooms G, Norman D. Intracranial vascular malformations: MR and CT imaging. *Radiology* **1985**;156:383–389
21. Lee BCP, Herzberg L, Zimmerman RD, Deck MDF. MR imaging of cerebral vascular malformations. *AJNR* **1985**;6:863–870
22. Gomori JM, Grossman RI, Goldberg HI, Zimmerman RA, Bilaniuk LT. Intracranial hematomas: imaging by high-field MR. *Radiology* **1985**;157:87–93
23. Sipponen JT, Sepponen RE, Sivula A. Nuclear magnetic resonance (NMR) imaging of intracerebral hemorrhage in the acute and resolving phases. *J Comput Assist Tomogr* **1983**;7:954–959
24. DeLaPaz RL, New PFJ, Buonanno FS, et al. NMR imaging of intracranial hemorrhage. *J Comput Assist Tomogr* **1984**;8:599–607
25. Bailes DR, Young IR, Thomas DJ, Straughan K, Bydder GM, Steiner RE. NMR imaging of the brain using spin-echo sequences. *Clin Radiol* **1982**;33:395–414
26. Brant-Zawadzki M, Davis PL, Crooks LE, et al. NMR demonstration of cerebral abnormalities: comparison with CT. *AJNR* **1983**;140:847–854
27. Pykett IL, Rosen BR, Buonanno FS, Brady TJ. Measurement of spin-lattice relaxation times in nuclear magnetic resonance imaging. *Phys Med Biol* **1983**;28:723–729
28. DiChiro G, Brooks RA, Girton ME, et al. Sequential MR studies of intracerebral hematomas in monkeys. *AJNR* **1986**;7:193–199
29. Holland BA, Kucharczyk W, Brant-Zawadzki M, Norman D, Haas DK, Harper PS. MR imaging of calcified intracranial lesions. *Radiology* **1985**;157:353–356
30. Oot RF, New PFJ, Rosen BR, Davis KR. The detection of intracranial calcifications by MR imaging. Presented at the 24th annual meeting of the American Society of Neuroradiology, San Diego, CA, January **1986**
31. Ahmadi J, Miller CA, Segall HD, Park S-H, Zee C-S, Becker RL. CT patterns in histopathologically complex cavernous hemangiomas. *AJNR* **1985**;6:389–393
32. Wilson CB, U HS, Domingue J. Microsurgical treatment of intracranial vascular malformations. *J Neurosurg* **1979**;51:446–454
33. Kjellberg RN, Hanamura T, Davis KR, Lyons SL, Adams RD. Bragg-Peak proton beam therapy for arteriovenous malformations of the brain. *N Engl J Med* **1983**;309:269–274